Original Article
Profiles of immune cell infiltration and immune-related genes in the tumor microenvironment of HNSCC with or without HPV infection

Dajie Zhou[1], Jing Wang[1], Junxin Wang[2], Xiangdong Liu[3]

[1]Department of Clinical Laboratory Center, Yantai Yuhuangding Hospital, Yantai 264000, Shandong, China; [2]Department of Clinical Medicine, Weifang Medical University, Weifang 261053, Shandong, China; [3]Department of Clinical Laboratory, Shandong Provincial Hospital Affiliated to Shandong First Medical University, Jinan 250021, Shandong, China

Abstract: Head and neck squamous cell carcinoma (HNSCC) are the sixth most common cancer type in the world. Human papillomavirus (HPV) infection is an emerging risk factor for HNSCC. Immune infiltration of HNSCC is linked to therapeutic results. This article aimed to decide whether variations in HPV status affect immune infiltration, molecular mechanism, and how these results vary in HNSCC patients. We investigated the tumor-infiltrating immune cells (TIICs) and immune-related gene differences between HPV (+) and HPV (-) HNSCC. The gene expression quantification data of HNSCC and their clinical information were download from the TCGA database. Immune-related genes have been linked to the ImmPort platform. After analyzed of 22 TIICs in the HNSCC tumor environment by CIBERSORT and further assessment, lower memory B cell and higher T cell regulatory were connected with better HPV (-) HNSCC outcome, higher activated memory CD4 T cell, higher T cell regulatory, and lower activated NK cell were linked with better HPV (+) result. We finally got five forms of immune genes (CAMP, EDNRB, NTS, CXCL9, LHB) associated with HNSCC progression. Higher expressions of CAMP, EDNRB, and NTS were associated with increased overall survival in HPV (-) patients. Higher expression of CXCL9 and lower expression of LHB contributed to increased overall survival of HPV (+) patients. There tend to be discrepancies in the cell structure of TIICs and immune-related genes in HPV (-) and HPV (+) HNSCC. These variances are typically too crucial for the therapeutic outcome of the patient and the development of the tumor. In specific, our sample established these candidate immune cells and immune-related genes as candidate reservoirs for further researches.

Keywords: HNSCC, human papillomavirus, tumor-infiltrating immune cells, immune-related gene, prognostic value

Introduction

Head and neck squamous cell carcinoma (HNSCC) are the sixth most common cancer type in the world. The latest statistics show that the annual incidence of HNSCC is 53,260 cases accounting for 3% of new cancers and 10,750 deaths per year, accounting for 1.78% of cancer deaths [1]. HPV (+) HNSCC cancers have recently risen in epidemiological research. A recent population-based analysis showed that HPV (+) HNSCC cancers rose by 225%, while HPV (-) HNSCC cancer incidence decreased by 50% [2]. In specific, p16 is a reliable marker for active HPV infections [3]. The discovery of possible molecular biomarkers or therapeutic targets to overcome HNSCC is therefore desperately needed.

Several studies of HPV-associated HNSCC have been reported. The tumor microenvironment can regulate tumor response to therapy. It is known that HPV (+) HNSCC is radiotherapy sensitive better than HPV (-) HNSCC. HPV promoted M1 polarization of macrophages by tumor cell secretion of IL-6, thereby increasing therapy sensitivity [4]. HPV infection affects cancer-related alternative splicing events (CASEs), and CASEs enriched in immune-related pathways were closely related to immune cell infiltration activity [5]. Hence, figuring the difference between HPV-positive and HPV-negative out is essential guidelines for treatment.

Emerging evidence revealed that TIICs, a significant component of the tumor microenvironment, play a critical part in cancer prognosis

and response to therapy [6]. Recently, Cell type Identification by Estimating Relative Subsets of RNA Transcripts (CIBERSORT), a powerful computational technique for measuring cell fractions from cancer tissue gene expression profiles, can use rigorous statistical optimization techniques to reliably predict 22 TIIC levels in large volumes of cancer samples. CIBERSORT has been successfully used to find TIICs landscapes and their associations with prognosis and immunotherapy efficacious in lung cancer, osteosarcoma, and acute myeloid leukemia [7-9].

This research gathered data on HPV (-) and HPV (+) expression of HNSCC tissue and their relative clinical data from the TCGA database. Twenty-two forms of HNSCC immune infiltration cells were analyzed using the CIBERSORT algorithm and certain immune cells were closely related to HPV (-) and HPV (+) HNSCC.

To increase immunotherapy efficacy, determining immune-associated prognostic biomarkers is especially pivotal. Here, we calculated the differentially expressed immune-related genes in HPV (-) and HPV (+) HNSCC tissues, function annotation, and their prognosis value of hub genes in the PPI network. Both of these outcomes may provide better guidance for understanding the different pathogenesis pathways and treatment responses between HPV-negative and HPV-positive HNSCC.

Methods

Data collection and processing

HNSCC samples gene expression quantification data of the HTSeq-FPKM type and corresponding clinical data were downloaded from TCGA (https://tcga-data.nci.nih.gov/tcga/) on February 2, 2020, including 502 HNSCC samples and 44 para-tumor tissues. We manually classified each piece into two groups: HPV (-) group and HPV (+) group. Finally, 72 HPV (-) samples and 30 HPV (+) samples were compared with these 44 control samples for further immune cell infiltration analysis and immune-related gene analysis. The patient profile data and clinical features of HNSCC are publicly available and available upon open access.

Analysis of the tumor microenvironment of TIICs in HNSCC tissues

In our study, the CIBERSORT method tested TIICs in HPV (-) and HPV (+) HNSCC tissues from the TCGA database. Twenty-two TIICs gene ex-

pression matrices were obtained from CIBERSORT. R software (version 3.5.3) package of e1071 (version 1.7-3), package of parallel (version 3.5.3), and bioconductor package of preprocessCore (version 3.10) were used to calculate the proportion of 22 TIICs in both HPV (-) and HPV (+) HNSCC tissues. Subsequently, the distribution of 22 immune cell subsets, including P-value, correlation coefficient and root mean squared error (RMSE), was determined. This will test the precision of the data. Therefore, samples with a CIBERSORT $P < 0.05$ as a cut-off value, only $P < 0.05$ samples were supposed for advance analysis. Additionally, the number of permutations of the preset signature matrix was 100. In the end, only 11 normal samples, 64 HPV (-) samples, and 22 HPV (+) samples were selected for further analysis.

Identification of immune-related differentially expressed genes in HPV (-) and HPV (+) HNSCC samples

To analyze immune-related DEGs in HNSCC tissues, the mRNA expression information of HNSCC patients was obtained from the TCGA data portal. Also, immune-associated genes were retrieved from the ImmPort platform (https://www.immport.org/). Differential immune-related mRNA expression of HPV (-) and HPV (+) HNSCC samples analyzed by bioconductor package of edgeR, these DEGs results visualized by R software package of gplots (version 3.0.1.2). DEGs between the data sets were obtained using |log2-fold change| ≥ 1.0 and $P < 0.05$ as a cut-off criterion.

Construction of a PPI network from immune-related DEGs

To interpret the various underlying protein associations of both HPV (-) and HPV (+) HNSCC tissues, a PPI network of immune-related DEGs was conducted using the STRING database (version 11) and reconstructed by Cytoscape software (version 3.7.2). The network verified interactions combined score < 0.9 nodes are omitted. To better know the relationship of these immune-related DEGs, Cytoscape's MCODE program was used to find closely related clusters of gene hubs. Only clusters with 10 or more nodes were chosen for further study.

Gene ontology and KEGG pathway enrichment analysis

Gene Ontology (GO) Biological Process term and Kyoto Encyclopedia of Genes and Genomes

(KEGG) pathway analysis were conducted using R software and DAVID database (https://david.ncifcrf.gov/). R packages of GO plot visualized GO enrichment analysis. Relevant enrichment of KEGG was analyzed by R packages of RSQLite, org.Hs.eg.db, clusterProfiler, visualized by Cytoscape software 3.7.2. GO terms, and KEGG pathways were selected correlation with immunity. *FDR* < 0.05 was used as the statistically significant cut-off.

Overall survival analysis

We combined every immune-related hub gene expression, patients' overall survival times, and live status of HPV (-) and HPV (+) HNSCC. The R package of survival was used to calculate the Kaplan-Meier survival curves, *P* < 0.05 was used as the statistically significant cut-off.

Statistical analysis

The different immune infiltration levels of each immune cell between the two groups were analyzed by the vioplot package in R version 3.5.2. The correlations among TIICs were analyzed with the corrplot package. Log-rank test was performed to compare Kaplan-Meier curves, which were used to play survival curves that reflect immune genes and immune cells association with corresponding clinical information. Wilcox test was executed to assess the differences of cell proportions between groups.

Results

The landscape of TIICs in HPV (-) and HPV (+) HNSCC tissues

CIBERSORT algorithm was used to screen out samples with CIBERSORT output *P* value less than 0.05 for research. As a result, only 11 normal samples, 64 HPV (-) and 22 HPV (+) samples were chosen for the CIBERSORT study (Supplementary Table 1). We plotted a bar plot to display the proportion of 22 immune cells in each sample (**Figure 1A**, **1B**). Then, a heat map of 22 immune cells was plotted, both HPV (-) and HPV (+) tissues relative to normal tissues (**Figure 1C**, **1D**). Furthermore, the correlation analysis found that the activated T cell CD4 memory had the strongest positive correlation with the T cell CD8 in the HPV (-) tissues, and the T cell CD8 had the strongest negative correlation with the M0 macrophage (**Figure 1E**).

Correlation matrix in HPV (+) tissues revealed that B-cell naive had the strongest positive correlation with B-cell memory, whereas Macrophage M2 had the strongest negative correlation with T-cell follicular helper (**Figure 1F**). These findings revealed a distinct TIICs between HPV (-) and HPV (+) HNSCC.

The different proportion of 22 TIICs in HPV (-) and HPV (+) tissues of HNSCC

Differences of 22 TIICs were compared between HPV (-) (N = 64) and HPV (+) (N = 22) HNSCC tissues and normal tissues (N = 11). The results show that Eosinophil cells were infiltrated differently in HPV (-) tissues (*p* value < 0.05) (**Figure 2A**). In contrast, activated NK cells, Monocytes cells, Macrophages M0 cells, resting Dendritic cells, Neutrophil cells were the principal infiltrated differently component in HPV (+) tissues (*p* value < 0.05) (**Figure 2B**). This difference in the proportion of TIICs, which may be a core feature of the distinct HNSCC pathogenesis of different HPV status.

Predictive value of TIICs in HPV (-) and HPV (+) tissues

Kaplan-Meier analysis was utilized to investigate the prognostic value of 22 TIICs in HPV (-) and HPV (+) tissues. In the results, we find that low expression level of regulatory T cells (*p* value = 0.005) and high expression level of memory B cells (*p* value = 0.023) were associated with poor prognosis in HPV (-) tissues (**Figure 3A**). In the HPV (+) tissues, low expression level of regulatory T cells (*p* value = 0.018) and activated memory CD4 T cells (*p* value = 0.001), as well as high expression level of activated NK cells (*p* value = 0.053) were closely associated with poor prognosis value (**Figure 3B**).

Data set acquisition and identification of differentially expressed immune-related genes

From the TCGA database, 72 HPV (-) samples and 30 HPV (+) samples were compared with those 44 standard samples for immune-related gene analysis. Between 72 HPV (-) and 44 normal tissues, 40 down-regulated and 193 up-regulated immune-related genes were present (**Figure 4A**). There were 193 down-regulated and 110 up-regulated immune-related genes within 30 HPV (+) and 44 natural tissues (**Figure**

Differences in HNSCC immune infiltration in various HPV status
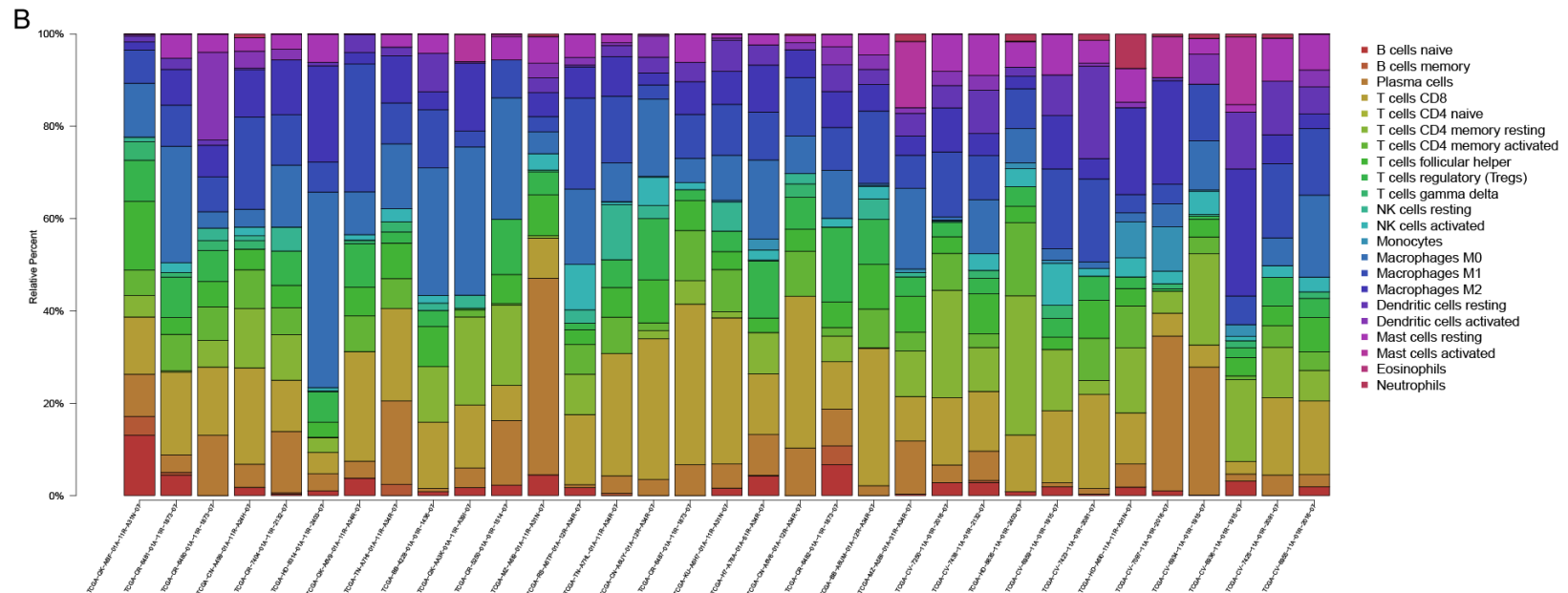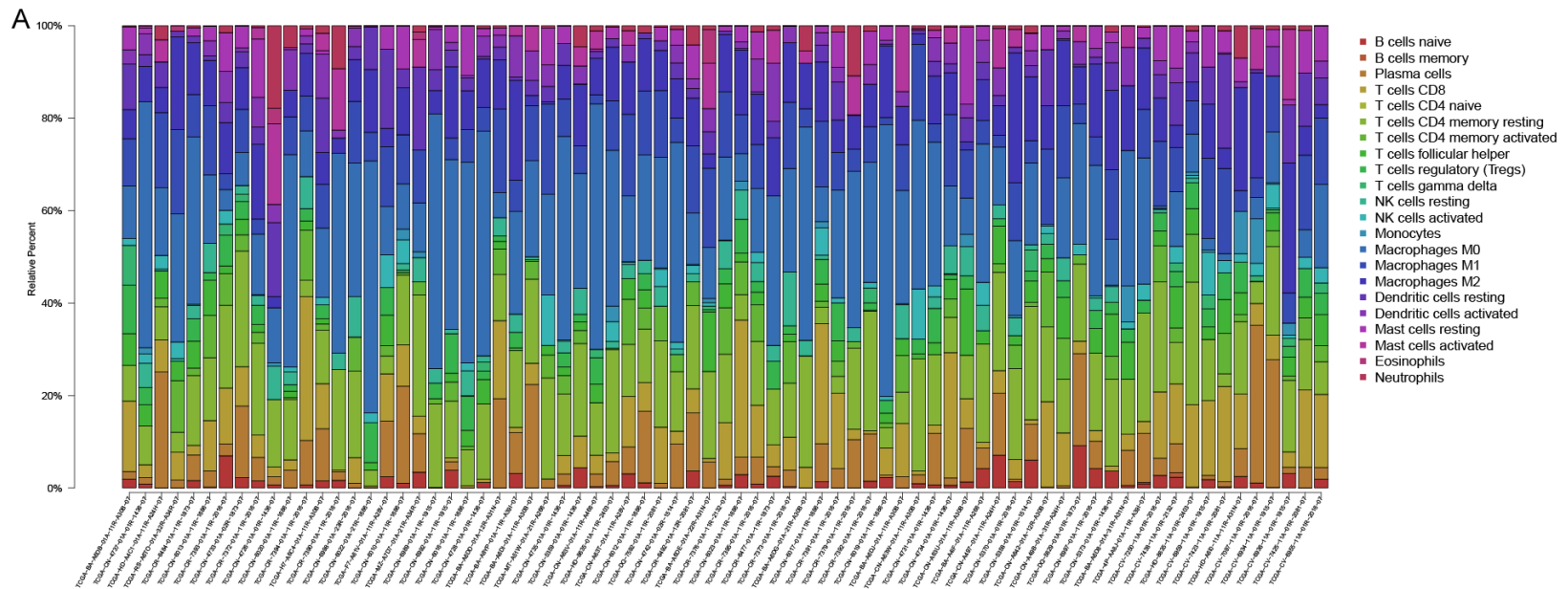
Differences in HNSCC immune infiltration in various HPV status
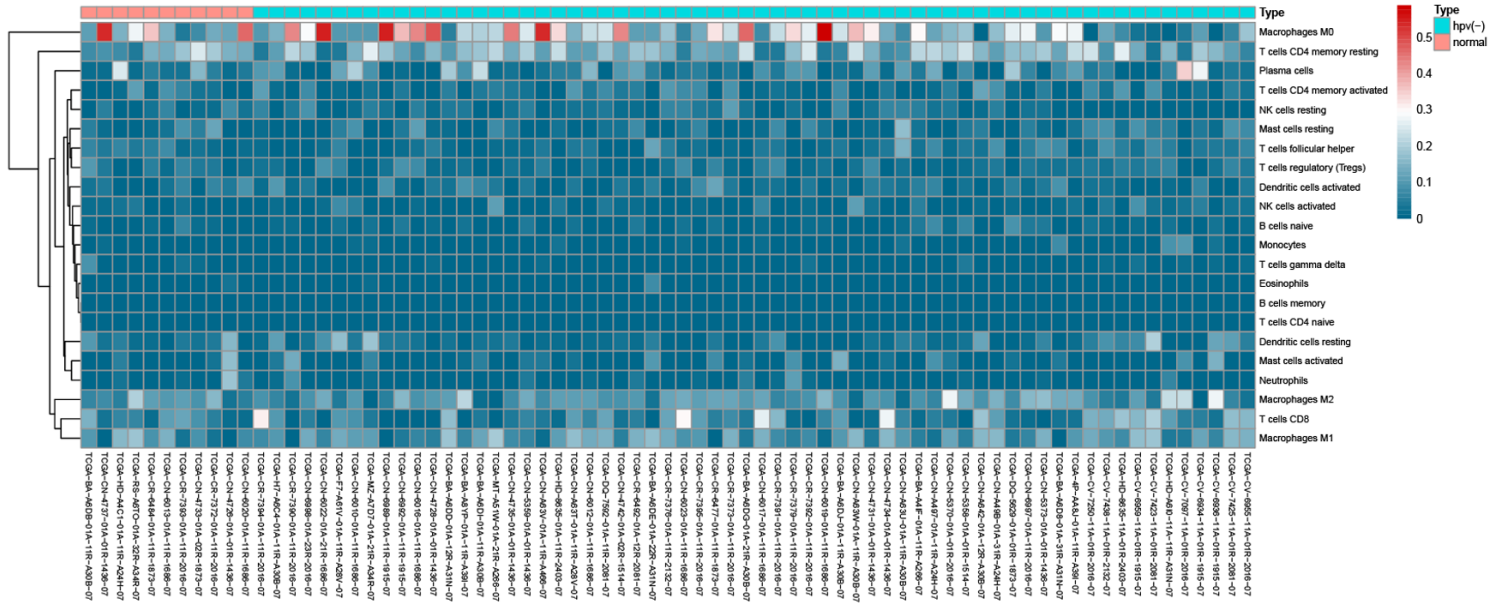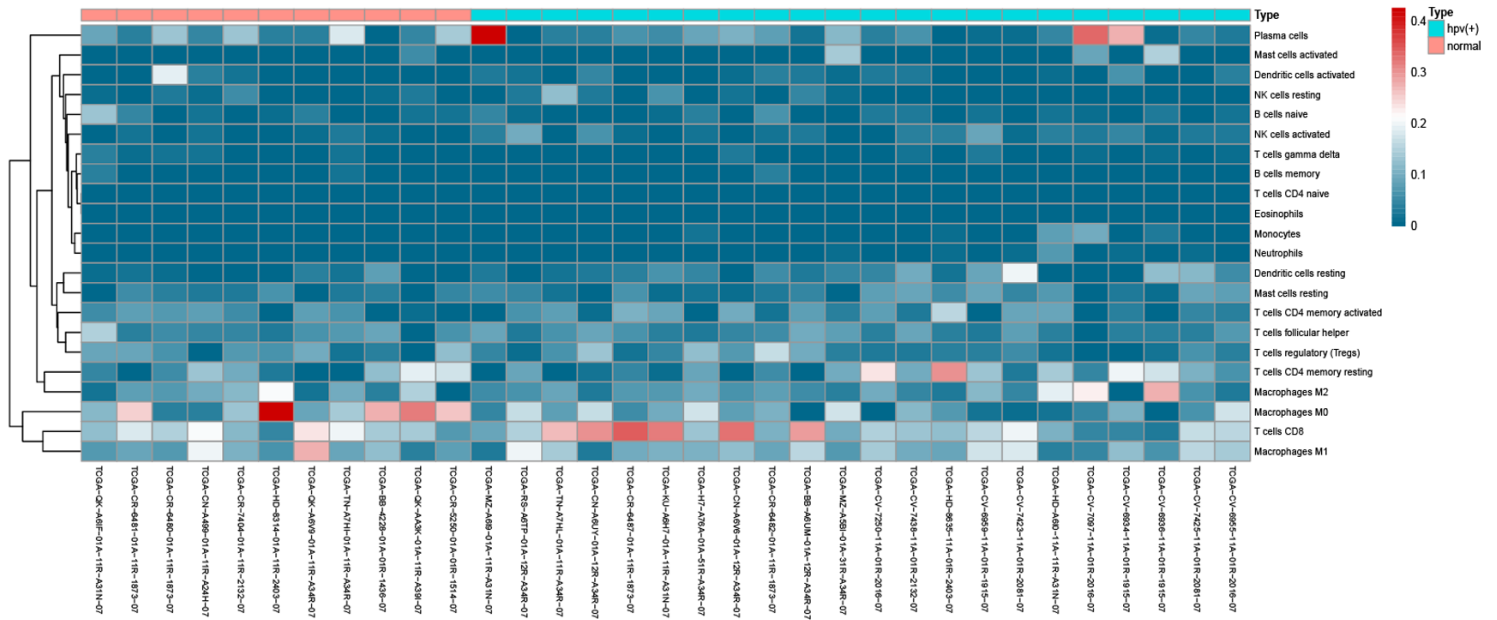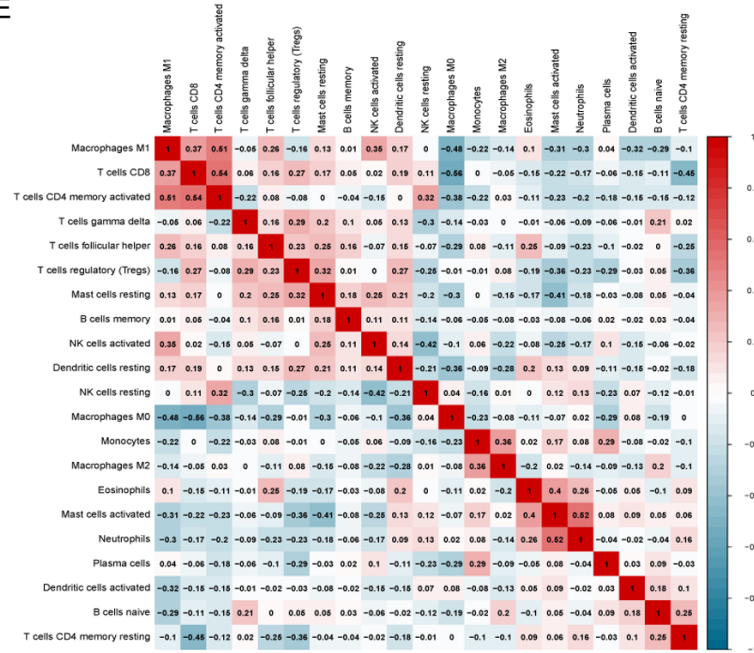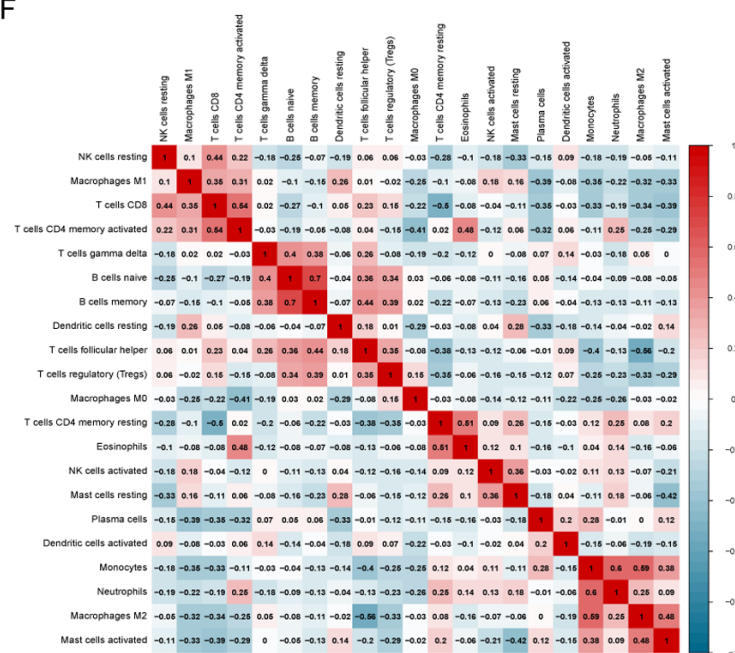
Figure 1. Composition of 22 TIICs in each sample in the TCGA cohort. A. Composition of TIICs in each 64 HPV (-) HNSCC and 11 normal samples. B. Composition of TIICs in each 22 HPV (+) HNSCC and 11 normal samples. C. A heatmap of the TIICs proportions in 64 HPV (-) HNSCC and 11 normal samples. D. A heatmap of the TIICs proportions in 22 HPV (+) HNSCC and 11 normal samples. E. Correlation matrix of TIICs proportions in 64 HPV (-) HNSCC. F. Correlation matrix of TIICs proportions in 22 HPV (+) HNSCC. Red represents high, white represents moderate, and blue represents low relativity.
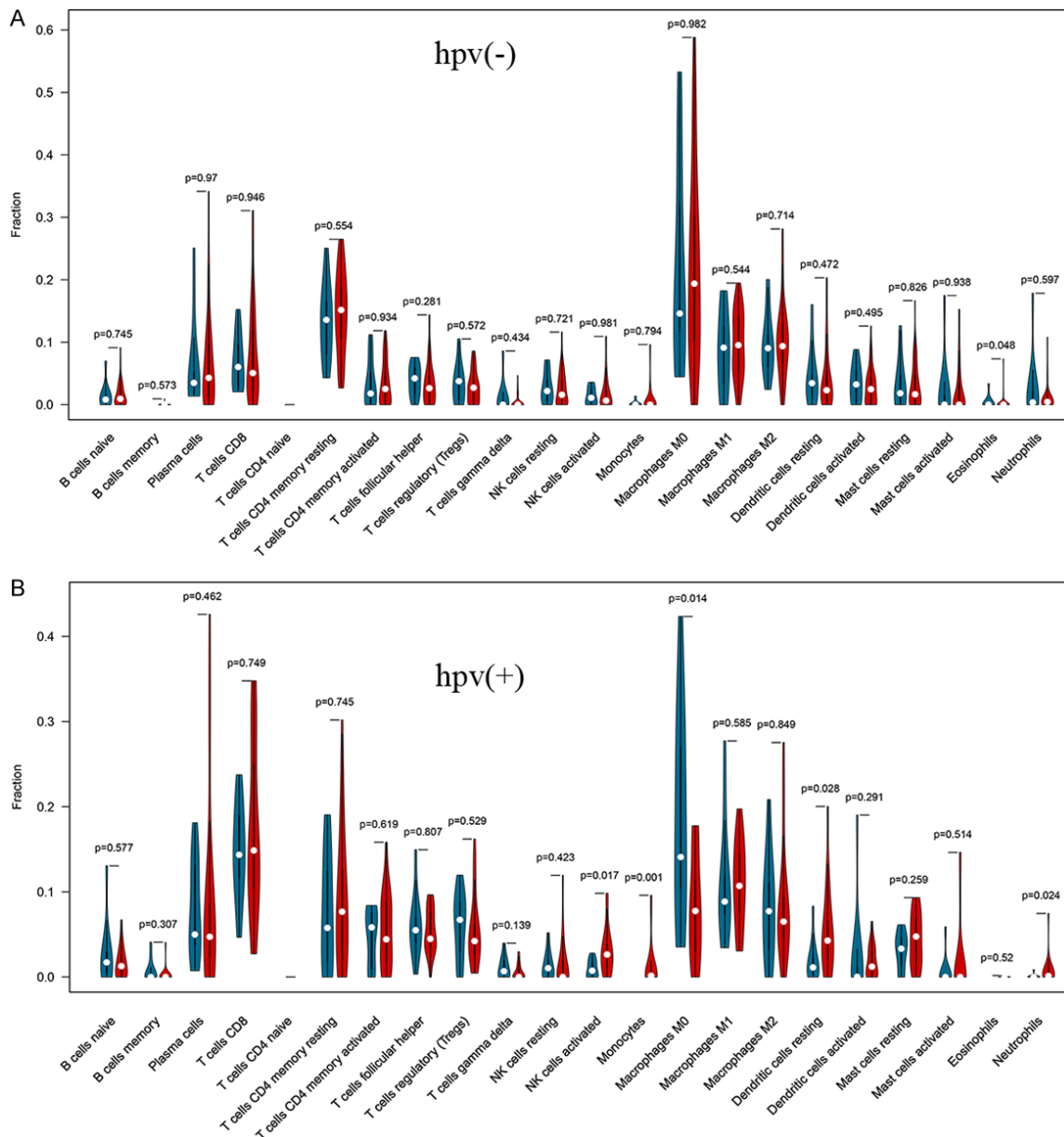
Figure 2. Violin plot comparing the proportions of TIICs between HNSCC and normal tissues. A. The proportions of TIICs between HPV (-) HNSCC and normal tissues. B. The proportions of TIICs between HPV (+) HNSCC and normal tissues. Red represents HNSCC tissues, and blue represents normal tissues. $P < 0.05$ represents statistical significance.

4B). The heat map of immune-related genes shows the differences between HPV (-) and HPV (+) tissues with normal tissues.

PPI network and function annotation analysis

As a result, we performed HPV (+) PPI network containing 302 nodes and 960 edges. We performed HPV (-) PPI network containing 232 nodes and 540 edges. We selected the most significant three modules of HPV (-) (**Figure 5A**)

and HPV (+) (**Figure 5B**) tissues for further analysis.

These significant module genes show a strong relationship with an immune response as well. The top four specifically immune-related GO terms and genes were selected in the HPV (-) category (**Figure 6A**) (**Tables 1** and **2**) (*FDR < 0.05*). In the HPV (+) category, the top 10 specifically immune-related GO words and genes were picked (**Figure 6B**) (*FDR < 0.05*). There
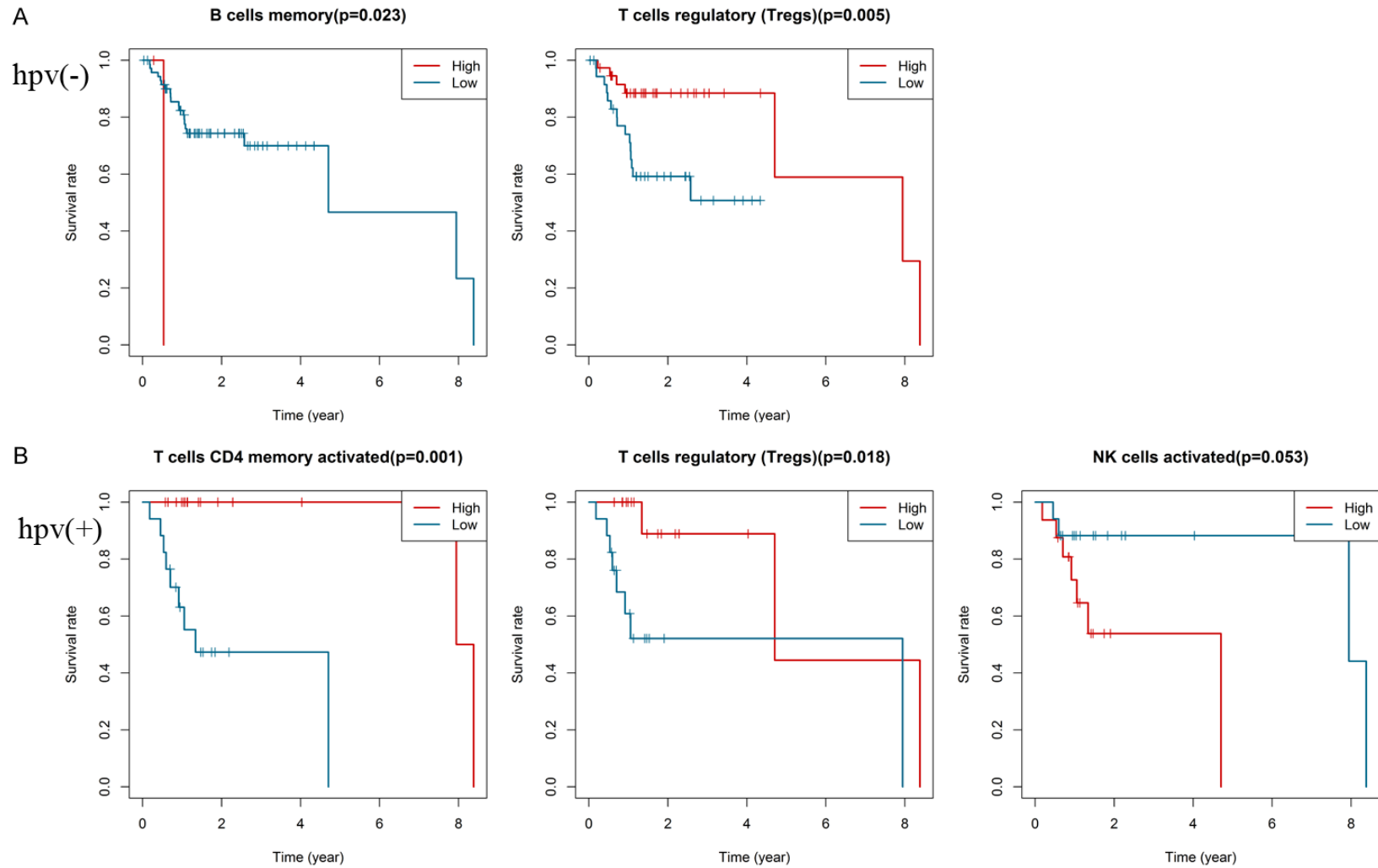
Figure 3. Prognostic value of TIICs in HPV (-)/(+) HNSCC by Kaplan-Meier analysis. A. Prognostic value of TIICs in HPV (-) HNSCC. B. Prognostic value of TIICs in HPV (+) HNSCC. *P* < 0.05 represents statistical significance.
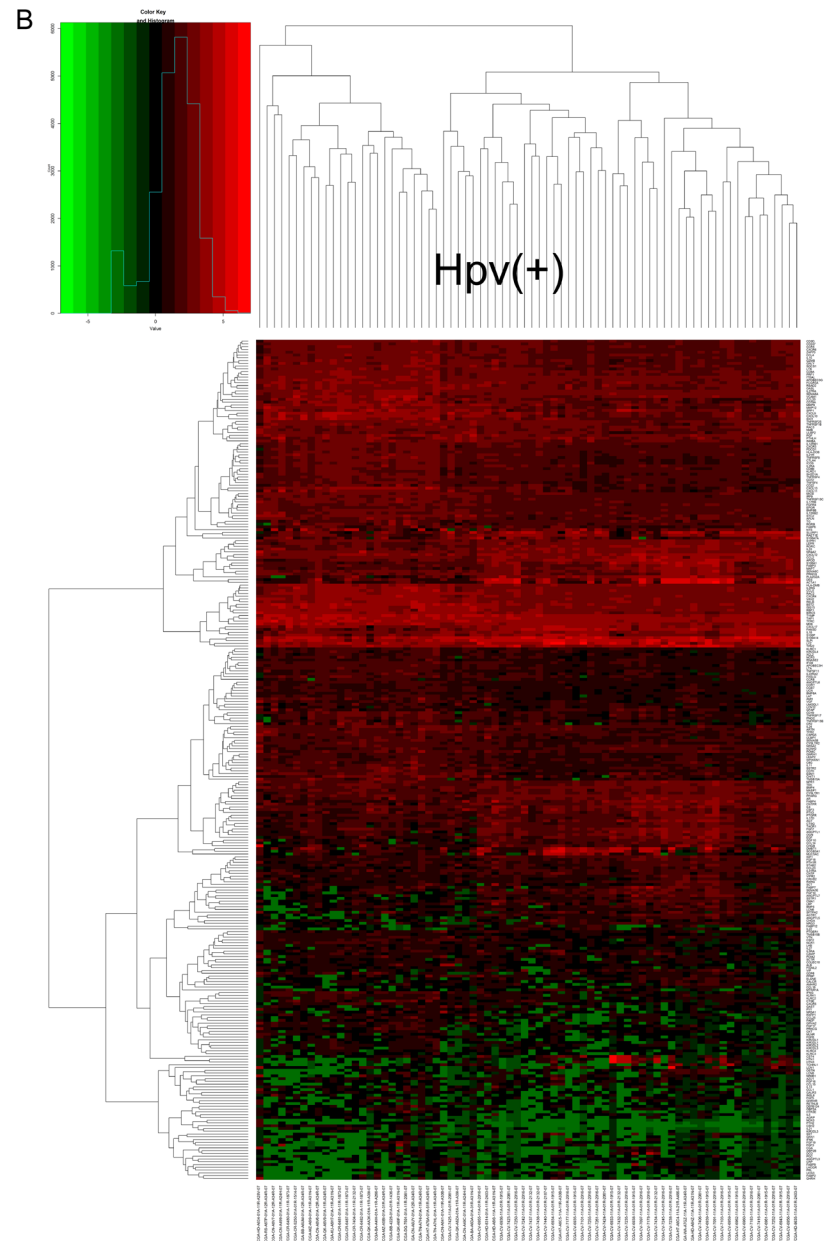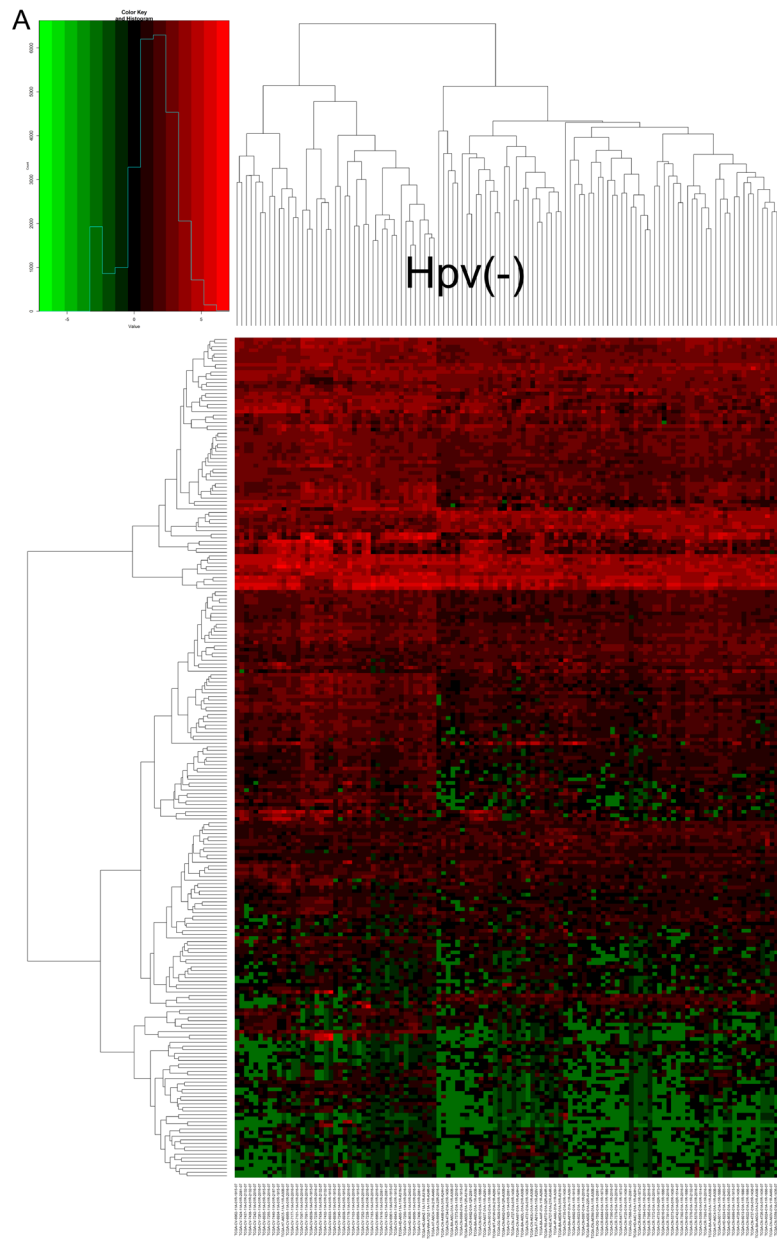
Differences in HNSCC immune infiltration in various HPV status

Figure 4. Clustered heat maps of the differentially expressed immune-related RNAs in HPV (-)/(+) HNSCC. A. Differentially expressed immune-related RNAs in HPV (-) HNSCC. B. Differentially expressed immune-related RNAs in HPV (+) HNSCC. Columns represent HPV (-)/(+) HNSCC samples, whereas rows represent immune-related RNAs, |log2-fold change| ≥ 1.0 and $P < 0.05$.
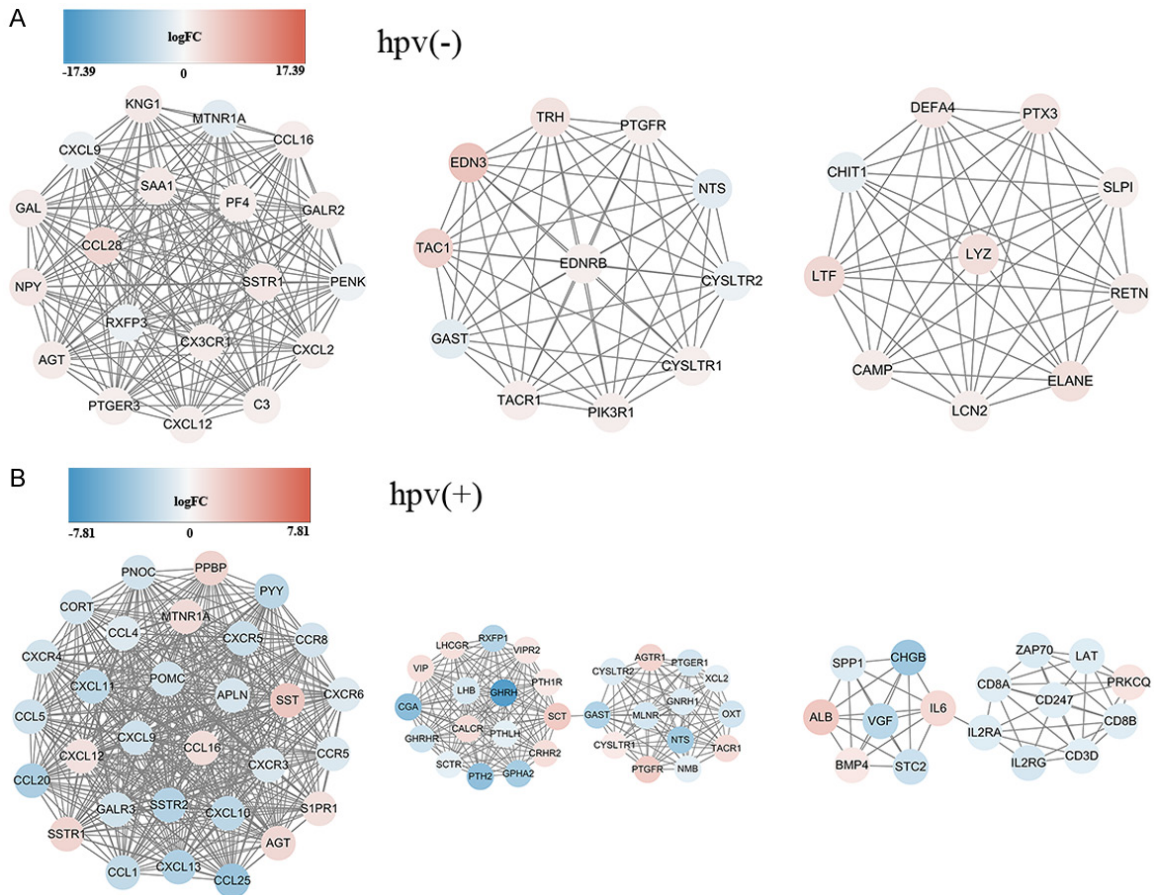
Figure 5. Top three immune-related gene modules of HPV (-)/(+) HNSCC samples extracted by MCODE. A. Immune-related gene modules of HPV (-) HNSCC. B. Immune-related gene modules of HPV (+) HNSCC.

were four common GO terms, chemokine-mediated signaling pathway, inflammatory response, chemokine activity, immune response, in HPV (-) and HPV (+) groups. Monocyte chemotaxis, T cell receptor complex, positive regulation of inflammatory response, positive regulation of leukocyte chemotaxis, lymphocyte chemotaxis, positive regulation of T cell migration were HPV (+) unique enrichment GO terms.

According to the KEGG pathway findings, several KEGG enrichments and associated genes varied between the HPV (-) and HPV (+) groups. The findings show that hsa04080, hsa04061, hsa04062, hsa04020, hsa04060, hsa04024 are common pathways for HPV (-) and HPV (+) groups. HPV (-) unique pathway was hsa04923, but in the HPV (+) group, there were a lot of

immune-related pathways, including hsa046-59, hsa04658, hsa05340, hsa04620, hsa04-660, hsa04672, hsa05235, and hsa04640, hsa04064, hsa04623, hsa04929, hsa05163, hsa04935. All enrichment results of the HPV (-) and HPV (+) groups were played in **Figure 6C** and **6D**, and pathways names were shown in **Tables 3** and **4** (*p adjust* < 0.05).

Specific immune-related genes correlated with survival in HPV (-) and HPV (+) HNSCC

After calculating all of the hub-genes in the PPI network, the survival curves of HNSCC patients with HPV (-) and HPV (+) groups were got and shown in **Figure 7**. For HPV (-) patients, a high level of CAMP, EDNRB, and NTS were associated with poor prognosis (**Figure 7A**). For HPV (+),

Differences in HNSCC immune infiltration in various HPV status

Figure 6. Significantly enriched GO terms and KEGG pathway analysis in HPV (-)/(+) HNSCC samples. A. GO terms and corresponding immune-genes analysis in HPV (-) HNSCC samples. B. GO terms and corresponding immune-genes analysis in HPV (+) HNSCC samples. C. KEGG pathway and corresponding immune-genes in HPV (-) HNSCC samples. D. KEGG pathway and corresponding immune-genes in HPV (+) HNSCC samples. The color key represents the corresponding GO terms. Red represents upregulation, and blue represents downregulation. The KEGG pathway and the immune gene in the networks are represented as round rectangles and circles, respectively. *FDR* < 0.05.

Differences in HNSCC immune infiltration in various HPV status

Table 1. Significantly enriched GO term of HPV (-) HNSCC

ID	Description	Gene	*P* adjust
GO:0006954	inflammatory response	KNG1, PTGER3, C3, TACR1, CXCL2, CXCL9, LYZ, TAC1, PF4, PTGFR, CCL16, GAL, CXCL12, PTX3	0.000
GO:0008009	chemokine activity	CXCL2, CXCL9, PF4, CCL16, CXCL12, CCL28	0.000
GO:0006955	immune response	C3, CYSLTR2, CXCL2, CXCL9, SLPI, PF4, CCL16, CXCL12, CCL28, CHIT1	0.000
GO:0070098	chemokine-mediated signaling pathway	CXCL2, CX3CR1, CXCL9, PF4, CCL16, CXCL12	0.000

Table 2. Significantly enriched GO term of HPV (+) HNSCC

ID	Description	Gene	*P* adjust
GO:0070098	chemokine-mediated signaling pathway	CCL1, CXCL9, CXCR3, CXCL11, CCL16, CCL5, CXCL12, CCL4, CXCL10, CCL25, CCR8, PPBP, CCR5, CCL20, CXCR5, CXCR4, CXCL13, CXCR6, XCL2	0.000
GO:0006954	inflammatory response	CCL1, TACR1, CXCL9, CXCR3, CXCL11, CCL5, CXCL12, CCL4, CXCL10, CCL25, CCL20, CXCR4, CXCR6, ZAP70, SPP1, PTGER1, IL6, IL2RA, PTGFR, CCL16, PRKCQ, LAT, PPBP, CCR5, CXCL13, XCL2	0.000
GO:0008009	chemokine activity	CCL1, CXCL9, CCL5, CCL16, CXCL11, CCL4, CXCL12, CXCL10, CCL25, CCL20, PPBP, CXCL13, XCL2	0.000
GO:0006955	immune response	IL6, IL2RA, CD8A, CYSLTR2, CD8B, CXCL9, CXCL11, CCL16, CCL5, CCL4, CXCL12, CXCL10, CCL25, CCR8, LAT, PPBP, CCR5, CCL20, CXCR5, CXCL13, ZAP70, IL2RG, APLN	0.000
GO:0002548	monocyte chemotaxis	CCL1, CCL25, IL6, CCL20, CCL5, CCL16, CCL4, XCL2	0.000
GO:0042101	T cell receptor complex	CD3D, CD8A, CD8B, CD247, ZAP70	0.000
GO:0050729	positive regulation of inflammatory response	CCL1, AGTR1, AGT, CCL5, CCL16, CCL4, XCL2	0.001
GO:0002690	positive regulation of leukocyte chemotaxis	IL6, PPBP, CXCL9, CXCL11, CXCL10	0.001
GO:0048247	lymphocyte chemotaxis	CCL1, CCL25, CCL20, CCL16, XCL2	0.009
GO:2000406	positive regulation of T cell migration	CCL20, CCL5, CXCL12, CXCL10	0.014

Table 3. Significantly enriched KEGG pathway of HPV (-) HNSCC

ID	Description	p adjust	counts
hsa04080	Neuroactive ligand-receptor interaction	0.000	20
hsa04061	Viral protein interaction with cytokine and cytokine receptor	0.000	7
hsa04062	Chemokine signaling pathway	0.000	8
hsa04020	Calcium signaling pathway	0.005	6
hsa04060	Cytokine-cytokine receptor interaction	0.006	7
hsa04923	Regulation of lipolysis in adipocytes	0.037	3
hsa04024	cAMP signaling pathway	0.042	5

Table 4. Significantly enriched KEGG pathway of HPV (+) HNSCC

ID	Description	p adjust	counts
hsa04080	Neuroactive ligand-receptor interaction	0.000	36
hsa04061	Viral protein interaction with cytokine and cytokine receptor	0.000	21
hsa04060	Cytokine-cytokine receptor interaction	0.000	23
hsa04062	Chemokine signaling pathway	0.000	19
hsa04659	Th17 cell differentiation	0.000	8
hsa04658	Th1 and Th2 cell differentiation	0.000	7
hsa04024	cAMP signaling pathway	0.000	10
hsa05340	Primary immunodeficiency	0.000	5
hsa04620	Toll-like receptor signaling pathway	0.000	7
hsa04660	T cell receptor signaling pathway	0.000	7
hsa04020	Calcium signaling pathway	0.002	8
hsa04672	Intestinal immune network for IgA production	0.008	4
hsa05235	PD-L1 expression and PD-1 checkpoint pathway in cancer	0.009	5
hsa04640	Hematopoietic cell lineage	0.013	5
hsa04064	NF-kappa B signaling pathway	0.015	5
hsa04623	Cytosolic DNA-sensing pathway	0.015	4
hsa04929	GnRH secretion	0.015	4
hsa05163	Human cytomegalovirus infection	0.021	7
hsa04935	Growth hormone synthesis, secretion and action	0.022	5

a high level of CXCL9 and low LHB levels were uniquely associated with a poor prognosis for HNSCC patients (**Figure 7B**). These immune-related genes likely played a role in the pathogenesis of HNSCC.

Discussion

Although many studies have been shown in HNSCC carcinogenesis, the mechanism of HPV infection-induced pathogenesis of HNSCC remains unclear. Detecting specific biomarkers and identifying better therapeutic targets, thus, plays a crucial role in conquering the different HPV status of HNSCC.

In our research, we investigated the 22 TIICs and immune-related gene differences between HPV (-) and HPV (+) HNSCC. Higher T cell regulations were connected with better both HPV (-) and HPV (+) patient outcomes. Lower memory B cell was uniquely related to better HPV (-) patient outcomes. While higher activated memory CD4 T cell and lower activated NK cell were uniquely connected with better HPV (+) patient outcomes. Then, we compared HPV (-), and HPV (+) differentially expressed immune-related genes. We got 191 unique immune-related genes in HPV (+) patients, 121 unique immune-related genes in HPV (-) patients. Finally, we got five immune genes (CAMP, EDNRB, NTS, CXCL9, LHB) that were tightly associated with HNSCC progression. Differences in HPV (-) and HPV (+) HNSCC appear to exist, and these alterations are mostly too be vital for patient clinical outcome and tumor progression.
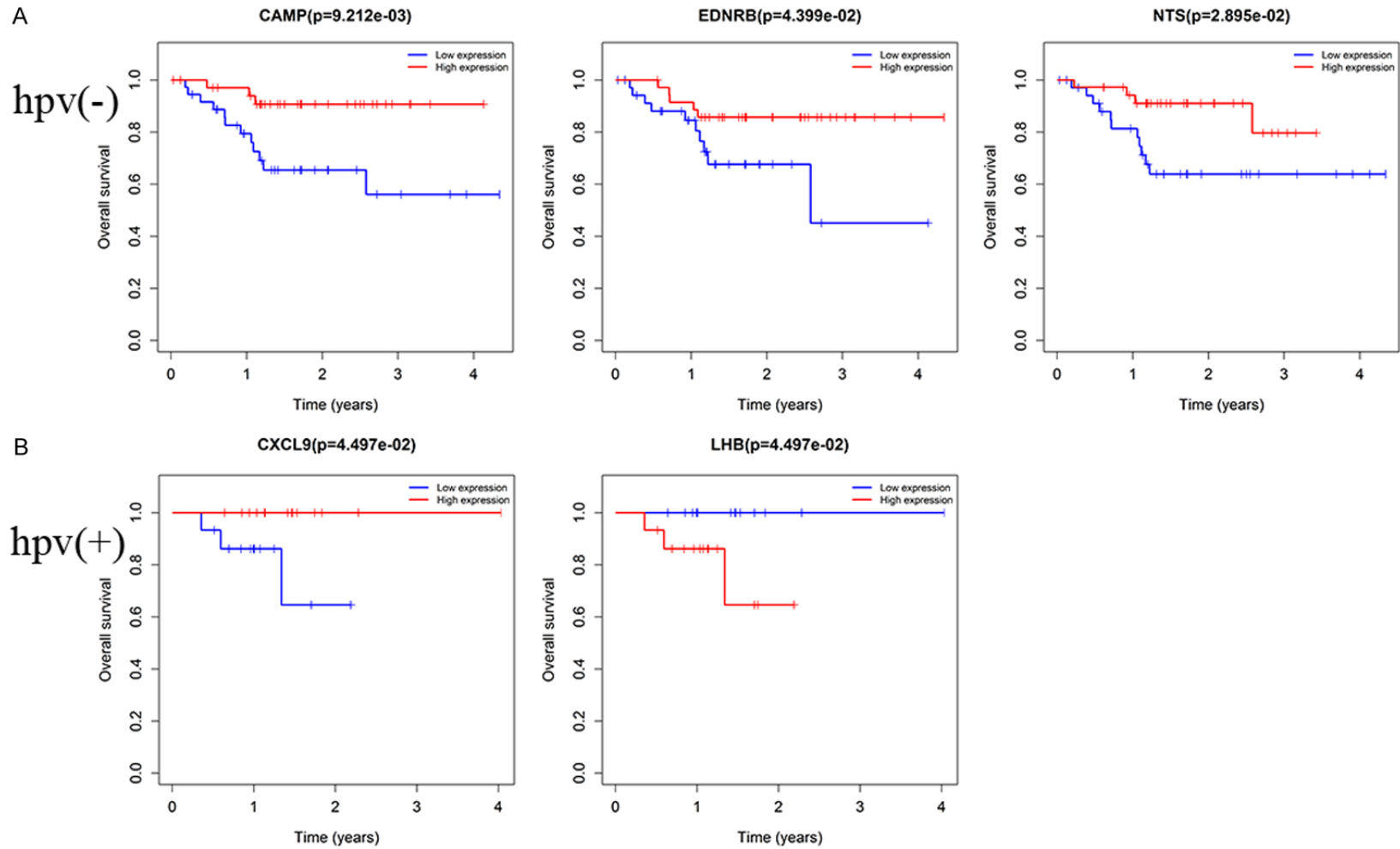
Figure 7. Overall survival analysis of immune-related RNAs of HPV (-)/(+) HNSCC. A. Prognostic value of immune-related RNAs in HPV (-) HNSCC. B. Prognostic value of immune-related RNAs in HPV (+) HNSCC. *P* < 0.05 represents statistical significance.

NK cells are cytotoxic lymphocytes of cancer immunotherapy ability. NK cell receptors, antagonists and active NK cell receptors regulate tumor growth in the tumor microenvironment. These NK cell receptors could be a candidate for cancer immunotherapy. Strengthened NK-cell-dependent cell-mediated cytotoxicity as an effective future approach to cancer treatment [10, 11]. NK cells possess an inborn capacity to recognise transformed cells that are essential to cancer immunosorption and antitumor immunity [12]. Yu deem that enhance NK cell cytotoxicity, activated by cytokines, immune checkpoint blockades, immunomodulatory drugs, to improve their killing activity toward gastric cancer [13]. An NK chimeric antigen receptor (CAR) cell was built by Lin et al. to improve the response of NK cell tumors. This CAR-NK cell greatly enhanced the capacity of NK cells to control many solid cancer cell lines in vitro, such as colorectal cancer [14]. In our results, the high expression level of activated NK cells poor prognosis in HPV (+) HNSCC. Thus, NK cells receptors and NK cell innate immune response plays a key role in the development of HPV (+) HNSCC.

Regulatory T cells are a crucial player for immune homeostasis. Regulatory T cells have been identified as a crucial part of immune evasion in many cancers, including HNSCC [15]. Many results show that regulatory T cells in tumor tissues are a reliable marker of prognosis, with a high level of regulatory T cells demonstrating a poor prognosis [16]. However, deLeeuw et al. also observed that increased regulatory T cell expression of the tumor microenvironment is associated with an improved prognosis of colorectal cancer [17]. Our findings suggest that high levels of regulatory T cells are associated with enhanced prognosis of HPV (-) and HPV (+) HNSCC. Thus, a sufficient number of regulatory T cell infiltration could be more conducive to HNSCC immunotherapy.

Memory B lymphocyte cells play a crucial role in immune responses for anticancer and cancer progression [18]. Lechner et al. found that memory B cells are enriched in the tumor microenvironment of HNSCC. The number of memory B cells in the HPV (-) HNSCC tumor microenvironment was slightly higher relative to HPV (+) HNSCC [19]. In our conclusion, we insight that high expression level of memory B cells relation to poor prognosis in HPV (-) HNSCC patients. Screening memory B cells may have driving importance for the HPV-HNSCC prognosis, and its mechanism of action requires further research.

The low expression level of activated memory CD4 T cells connected with poor prognosis in HPV (+) HNSCC. Pengbo et al. observed that the low proportion of active CD4 memory T cells was closely correlated with overall radiotherapy survival in many cancers [20]. Egeland et al. have demonstrated a clear association between activated CD4 memory T cells and M1 macrophages associated with ER status breast cancers that provide a high degree of inflammation [21]. From the perspective of activated memory CD4 T cell infiltration, the mechanism leading to the weaker prognosis of HPV (+) HNSCC remains to be studied.

EDNRB system has also been uncovered to influence many cellular functions in correlation with cancer genesis. Gu et al. showed that EDNRB expression is lower in primary cancer than the advanced tumor in breast cancer [22]. Fu et al. found that the proliferation and apoptosis of bladder cancer cells were regulated by EDNRB expression [23]. Masamichi et al. also found that the combination methylated gene of HOXA9 and EDNRB was the most useful indicator of HNSCC patients' poor recurrence-free survival [24]. Juliana exposed that EDNRB methylation is a valuable biomarker for oral cancer in a prospective study [25]. Our study has showed that high-level EDNRB expression is associated with poor HPV (-) HNSCC prognosis. These findings have shown that EDNRB can be especially useful in clinical screening of HPV (-) HNSCC.

Neurotensin (NTS) is involved in developing diverse tumors and is considered prospective targets for tumor therapy. Kwan et al. observed that CD133 (+) hepatocellular carcinoma tumor-initiating cells facilitate tumorigenesis by NTS-induced IL-8/CXCL1 signaling cascade stimulation [26]. Early research Ouyang et al. found that the NTS/NTSR1 signaling pathway facilitates glioblastoma development and as a biomarker indicates poor prognosis for patients with glioma [27]. Our results revealed that a high level of NTS is associated with poor prognosis in HPV (-) HNSCC patients. However, there are few studies about NTS in HNSCC develop-

ment. Considering its unique role in HPV (-) patients, we believe that NTS weighed heavily in developing HPV (-) HNSCC.

Chemokine shows a crucial role in the progression of several human cancers. Pein et al. uncovered that breast cancer cells secreting IL-1 induce CXCL9 production, fueling breast cancer lung metastases [28]. CXCL9 decreased CD8+ cytotoxic T lymphocytes in the tumor microenvironment of pancreatic adenocarcinoma and was associated with poor survival in patients [29]. Wang et al. data run a new mechanism, CD8+ T cells infiltrating and IFNγ-related genes CXCL9 upregulation, by which HPV infected cells escape host immunity [30]. Our data also revealed that a high level of CXCL9 expression unique associated with a poor prognosis for HPV (+) HNSCC patients. For CXCL9, there are major variations in HPV (+) HNSCC and it is hoped that it can be used as a drug candidate for diagnosis and treatment.

GO, and KEGG pathway used to weigh the enriched biological functions. Many of the unique pathways, Toll-like receptor signaling pathway, T cell receptor signaling pathway, PD-L1 expression and PD-1 checkpoint pathway in cancer, NF-kappa B signaling pathway, et al., were enriched in HPV (+) HNSCC. Therefore, the KEGG results might support that HPV (+) plays crucial parts via those pathways in HNSCC. Szczepanski et al. found that Toll-like receptor 4 enhanced HNSCC proliferation, induced nuclear NF-κB translocation, and protected tumor cells from immune attack [31]. All the results help to suggest that the development of immunotherapies for HPV (+) HNSCC.

Additionally, there were diverse limitations to our study. Just a limited number of HPV-infected HNSCC patients are available in the TCGA database, thus verification by in vivo and in vitro studies and other datasets is required for further research. In conclusion, we determined the differences between TIICs and immune-related genes as well as their functions between HPV (+) and HPV (-) HNSCC. Differences in TIICs and immune genes in HPV (-) and HPV (+) HNSCC may be crucial in immune responses for anticancer activity and therapy target for various HPV infection status patients.

Address correspondence to: Dr. Xiangdong Liu, Department of Clinical Laboratory, Shandong Provincial Hospital Affiliated to Shandong First Medical University, No. 324, Jingwu Weiqi Road, Jinan 250021, Shandong, China. Tel: +86-15168887036; E-mail: x__liu@126.com

References

[1] Siegel RL, Miller KD and Jemal A. Cancer statistics, 2020. CA Cancer J Clin 2020; 70: 7-30.

[2] Chaturvedi AK, Engels EA, Pfeiffer RM, Hernandez BY, Xiao W, Kim E, Jiang B, Goodman MT, Sibug-Saber M, Cozen W, Liu L, Lynch CF, Wentzensen N, Jordan RC, Altekruse S, Anderson WF, Rosenberg PS and Gillison ML. Human papillomavirus and rising oropharyngeal cancer incidence in the United States. J Clin Oncol 2011; 29: 4294-4301.

[3] Freitag J, Wald T, Kuhnt T, Gradistanac T, Kolb M, Dietz A, Wiegand S and Wichmann G. Extracapsular extension of neck nodes and absence of human papillomavirus 16-DNA are predictors of impaired survival in p16-positive oropharyngeal squamous cell carcinoma. Cancer 2020; 126: 1856-1872.

[4] Chen XH, Fu EH, Lou HH, Mao XH, Yan BQ, Tong FJ, Sun J and Wei LL. IL-6 induced M1 type macrophage polarization increases radiosensitivity in HPV positive head and neck cancer. Cancer Lett 2019; 456: 69-79.

[5] Li ZX, Zheng ZQ, Wei ZH, Zhang LL, Lin FL, Liu RQ, Huang XD, Lv JW, Chen FP, He XJ, Guan JL, Ma J, Zhou GQ and Sun Y. Comprehensive characterization of the alternative splicing landscape in head and neck squamous cell carcinoma reveals novel events associated with tumorigenesis and the immune microenvironment. Theranostics 2019; 9: 7648-7665.

[6] Wang C, Zhou X, Li WT, Li MY, Tu TY, Ba XM, Wu YY, Huang Z, Fan GT, Zhou GX, Wu SJ, Zhao JN, Zhang JF and Chen JN. Macrophage migration inhibitory factor promotes osteosarcoma growth and lung metastasis through activating the RAS/MAPK pathway. Cancer Lett 2017; 403: 271-279.

[7] Zhang K, Hong XH, Song ZB, Xu Y, Li CC, Wang GQ, Zhang YZ, Zhao XC, Zhao ZY, Zhao J, Huang ML, Huang DP, Qi C, Gao C, Cai SL, Gu FF, Hu Y, Xu CW, Wang WX, Lou ZK, Zhang Y and Liu L. Identification of deleterious NOTCH mutation as novel predictor to efficacious immunotherapy in NSCLC. Clin Cancer Res 2020; 26: 3649-3661.

[8] Zhang C, Zheng JH, Lin ZH, Lv HY, Ye ZM, Chen YP and Zhang XY. Profiles of immune cell infiltration and immune-related genes in the tumor microenvironment of osteosarcoma. Aging 2020; 12: 3486-3501.

[9] Xu ZJ, Gu Y, Wang CZ, Jin Y, Wen XM, Ma JC, Tang LJ, Mao ZW, Qian J and Lin J. The M2 macrophage marker CD206: a novel prognostic indicator for acute myeloid leukemia. Oncoimmunology 2020; 9: 1683347.

[10] Guillerey C, Huntington ND and Smyth MJ. Targeting natural killer cells in cancer immunotherapy. Nat Immunol 2016; 17: 1025-1036.

[11] Chiossone L, Dumas PY, Vienne M and Vivier E. Natural killer cells and other innate lymphoid cells in cancer. Nat Rev Immunol 2018; 18: 671-688.

[12] Souza-Fonseca-Guimaraes F, Cursons J and Huntington ND. The emergence of natural killer cells as a major target in cancer immunotherapy. Trends Immunol 2019; 40: 142-158.

[13] Du Y and Wei Y. Therapeutic potential of natural killer cells in gastric cancer. Front Immunol 2019; 9: 3095-3095.

[14] Xiao L, Cen D, Gan H, Sun Y, Huang N, Xiong H, Jin Q, Su L, Liu X, Wang K, Yan G, Dong T, Wu S, Zhou P, Zhang J, Liang W, Ren J, Teng Y, Chen C and Xu XH. Adoptive transfer of NKG2D CAR mRNA-engineered natural killer cells in colorectal cancer patients. Mol Ther 2019; 27: 1114-1125.

[15] Jie HB, Gildener-Leapman N, Li J, Srivastava RM, Gibson SP, Whiteside TL and Ferris RL. Intratumoral regulatory T cells upregulate immunosuppressive molecules in head and neck cancer patients. Br J Cancer 2013; 109: 2629-2635.

[16] Tanaka A and Sakaguchi S. Regulatory T cells in cancer immunotherapy. Cell Res 2017; 27: 109-118.

[17] deLeeuw RJ, Kost SE, Kakal JA and Nelson BH. The prognostic value of FoxP3+ tumor-infiltrating lymphocytes in cancer: a critical review of the literature. Clin Cancer Res 2012; 18: 3022.

[18] Garaud S, Buisseret L, Solinas C, Gu-Trantien C, de Wind A, Van den Eynden G, Naveaux C, Lodewyckx JN, Boisson A, Duvillier H, Craciun L, Ameye L, Veys I, Paesmans M, Larsimont D, Piccart-Gebhart M and Willard-Gallo K. Tumor infiltrating B-cells signal functional humoral immune responses in breast cancer. JCI insight 2019; 5: e129641.

[19] Lechner A, Schlößer HA, Thelen M, Wennhold K, Rothschild SI, Gilles R, Quaas A, Siefer OG, Huebbers CU, Cukuroglu E, Göke J, Hillmer A, Gathof B, Meyer MF, Klussmann JP, Shimabukuro-Vornhagen A, Theurich S, Beutner D and von Bergwelt-Baildon M. Tumor-associated B cells and humoral immune response in head and neck squamous cell carcinoma. Oncoimmunology 2019; 8: 1535293-1535293.

[20] Wen PB, Gao Y, Chen B, Qi XJ, Hu GS, Xu A, Xia JF, Wu LJ, Lu HY and Zhao GP. Pan-cancer analysis of radiotherapy benefits and immune infiltration in multiple human cancers. Cancers 2020; 12: 957.

[21] Egeland NG, Jonsdottir K, Aure MR, Sahlberg K, Kristensen VN, Cronin-Fenton D, Skaland I, Gudlaugsson E, Baak JPA and Janssen EAM. MiR-18a and miR-18b are expressed in the stroma of oestrogen receptor alpha negative breast cancers. BMC Cancer 2020; 20: 377-377.

[22] Gu X, Han S, Cui M, Xue J, Ai L, Sun L, Zhu X, Wang Y and Liu C. Knockdown of endothelin receptor B inhibits the progression of triple-negative breast cancer. Ann N Y Acad Sci 2019; 1448: 5-18.

[23] Fu W, Wu X, Yang Z and Mi H. The effect of miR-124-3p on cell proliferation and apoptosis in bladder cancer by targeting EDNRB. Arch Med Sci 2019; 15: 1154-1162.

[24] Hayashi M, Wu G, Roh J-L, Chang X, Li X, Ahn J, Goldsmith M, Khan Z, Bishop J, Zhang Z, Zhou XC, Richmon J, Agrawal N and Koch WM. Correlation of gene methylation in surgical margin imprints with locoregional recurrence in head and neck squamous cell carcinoma. Cancer 2015; 121: 1957-1965.

[25] Schussel J, Zhou XC, Zhang Z, Pattani K, Bermudez F, Jean-Charles G, McCaffrey T, Padhya T, Phelan J, Spivakovsky S, Brait M, Li R, Bowne HY, Goldberg JD, Rolnitzky L, Robbins M, Kerr AR, Sirois D and Califano JA. EDNRB and DCC salivary rinse hypermethylation has a similar performance as expert clinical examination in discrimination of oral cancer/dysplasia versus benign lesions. Clin Cancer Res 2013; 19: 3268-3275.

[26] Tang KH, Ma S, Lee TK, Chan YP, Kwan PS, Tong CM, Ng IO, Man K, To KF, Lai PB, Lo CM, Guan XY and Chan KW. CD133+ liver tumor-initiating cells promote tumor angiogenesis, growth, and self-renewal through neurotensin/interleukin-8/CXCL1 signaling. Hepatology 2012; 55: 807-820.

[27] Ouyang Q, Chen G, Zhou J, Li L, Dong Z, Yang R, Xu L, Cui H, Xu M and Yi L. Neurotensin signal-

ing stimulates glioblastoma cell proliferation by upregulating c-Myc and inhibiting miR-29b-1 and miR-129-3p. Neuro Oncol 2016; 18: 216-226.

[28] Pein M, Insua-Rodríguez J, Hongu T, Riedel A, Meier J, Wiedmann L, Decker K, Essers MAG, Sinn HP, Spaich S, Sütterlin M, Schneeweiss A, Trumpp A and Oskarsson T. Metastasis-initiating cells induce and exploit a fibroblast niche to fuel malignant colonization of the lungs. Nat Commun 2020; 11: 1494-1494.

[29] Gao HF, Cheng CS, Tang J, Li Y, Chen H, Meng ZQ, Chen Z and Chen LY. CXCL9 chemokine promotes the progression of human pancreatic adenocarcinoma through STAT3-dependent cytotoxic T lymphocyte suppression. Aging 2020; 12: 502-517.

[30] Wang W, Uberoi A, Spurgeon M, Gronski E, Majerciak V, Lobanov A, Hayes M, Loke A, Zheng ZM and Lambert PF. Stress keratin 17 enhances papillomavirus infection-induced disease by downregulating T cell recruitment. PLoS Pathog 2020; 16: e1008206-e1008206.

[31] Szczepanski MJ, Czystowska M, Szajnik M, Harasymczuk M, Boyiadzis M, Kruk-Zagajewska A, Szyfter W, Zeromski J and Whiteside TL. Triggering of Toll-like receptor 4 expressed on human head and neck squamous cell carcinoma promotes tumor development and protects the tumor from immune attack. Cancer Res 2009; 69: 3105-3113.